JOURNAL OF AGRICULTURAL AND FOOD CHEMISTRY

Chemical Imaging of Microstructures of Plant Tissues within Cellular Dimension Using Synchrotron Infrared Microspectroscopy

PEIQIANG YU,*,† JOHN J. MCKINNON,† COLLEEN R. CHRISTENSEN,‡,§ DAVID A. CHRISTENSEN,† NEBOJSA S. MARINKOVIC,|| AND LISA M. MILLER||

College of Agriculture, University of Saskatchewan, 51 Campus Drive, Saskatoon, S7N 5A8, Canada, BioMedical Imaging Group, Saskatoon, S7K 6M6, Canada, and National Synchrotron Light Source, Brookhaven National Laboratory, BNL-NSLS Building 725 D, Upton, New York 11973

Synchrotron radiation-based Fourier transform infrared microspectroscopy (SR-FTIR) is an advanced bioanalytical technique capable of exploring the chemistry within microstructures of plant and animal tissues with a high signal to noise ratio at high ultraspatial resolutions (3−10 μm) without destruction of the intrinsic structures of a tissue. This technique is able to provide information relating to the quantity, composition, structure, and distribution of chemical constituents and functional groups in a tissue. The objective of this study was to illustrate how the SR-FTIR technique can be used to image inherent structures of plant tissues on a cellular level (pixel size, ~10 μm × 10 μm). The results showed that with the extremely bright synchrotron light, spectra with high signal to noise ratios were obtained from areas as small as 10 μm × 10 μm in the plant tissue, which allowed us to "see" plant tissue in a chemical sense on a cellular level. The ultraspatial resolved imaging of plant tissues by stepping in pixel-sized increments was obtained. Chemical distributions of plant tissues such as lignin, cellulose, protein, lipid, and total carbohydrate could be mapped. These images revealed the chemical information of plant intrinsic structure. In conclusion, SR-FTIR can provide chemical and functional characteristics of plant tissue at high ultraspatial resolutions. The SR-FTIR microspectroscopic images can generate spatially localized functional group and chemical information within cellular dimensions.

KEYWORDS: Synchrotron; infrared microspectroscopy; chemical imaging; plant tissue; feed chemistry; ultraspatial resolutions

INTRODUCTION

Traditional analytical chemistry usually looks for a specific known component through homogenization of the tissue and separation of the components of interest from the complex matrix. As a result, the information about the spatial origin and distribution of the component of interest is lost and the object of the analysis is destroyed (*1*).

Recently, an advanced bioanalytical technique—synchrotron radiation-based Fourier transform infrared microspectroscopy (SR-FTIR)—has been emerging (*2*). This technique, taking advantage of synchrotron light brightness (which is usually 100−1000 times brighter than a conventional globar source) and small effective source size is capable of exploring the molecular chemistry within microstructures with high signal to noise ratios at high spatial resolutions as fine as 3−10 μm (*3*−*7*). This technique can encompass a wider spectral range so that more detailed structural information can be extracted. It can be used to detect information of ultrastructural chemistry by

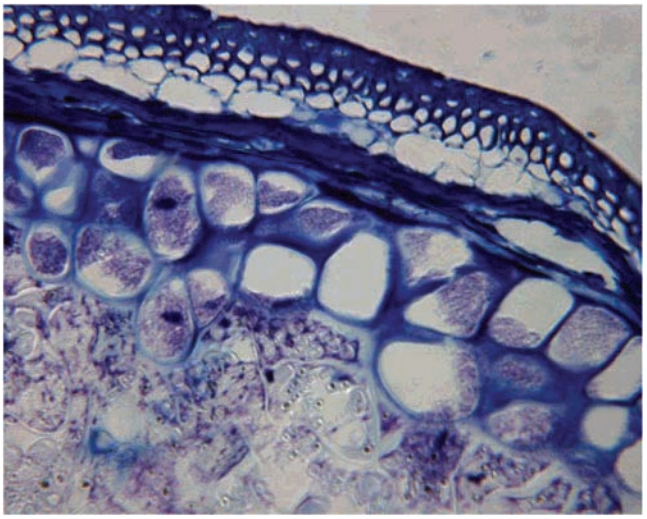

Figure 1. Photomicrograph of cross-section of barley (cv. Harrington) seed showing the intrinsic structure of the pericarp (outside of seed coat), seed coat, aleurone, and endosperm (magnification, 10 × 40).

* To whom correspondence should be addressed. Tel: +1 306 966 4132. E-mail: yupe@sask.usask.ca.
† University of Saskatchewan.
‡ BioMedical Imaging Group.
§ Present address: BioSynch Inc., 1305 10th Street, Saskatoon, S7H OJ2, Canada.
|| Brookhaven National Laboratory.

10.1021/jf034654d CCC: $25.00
Published on Web 08/26/2003

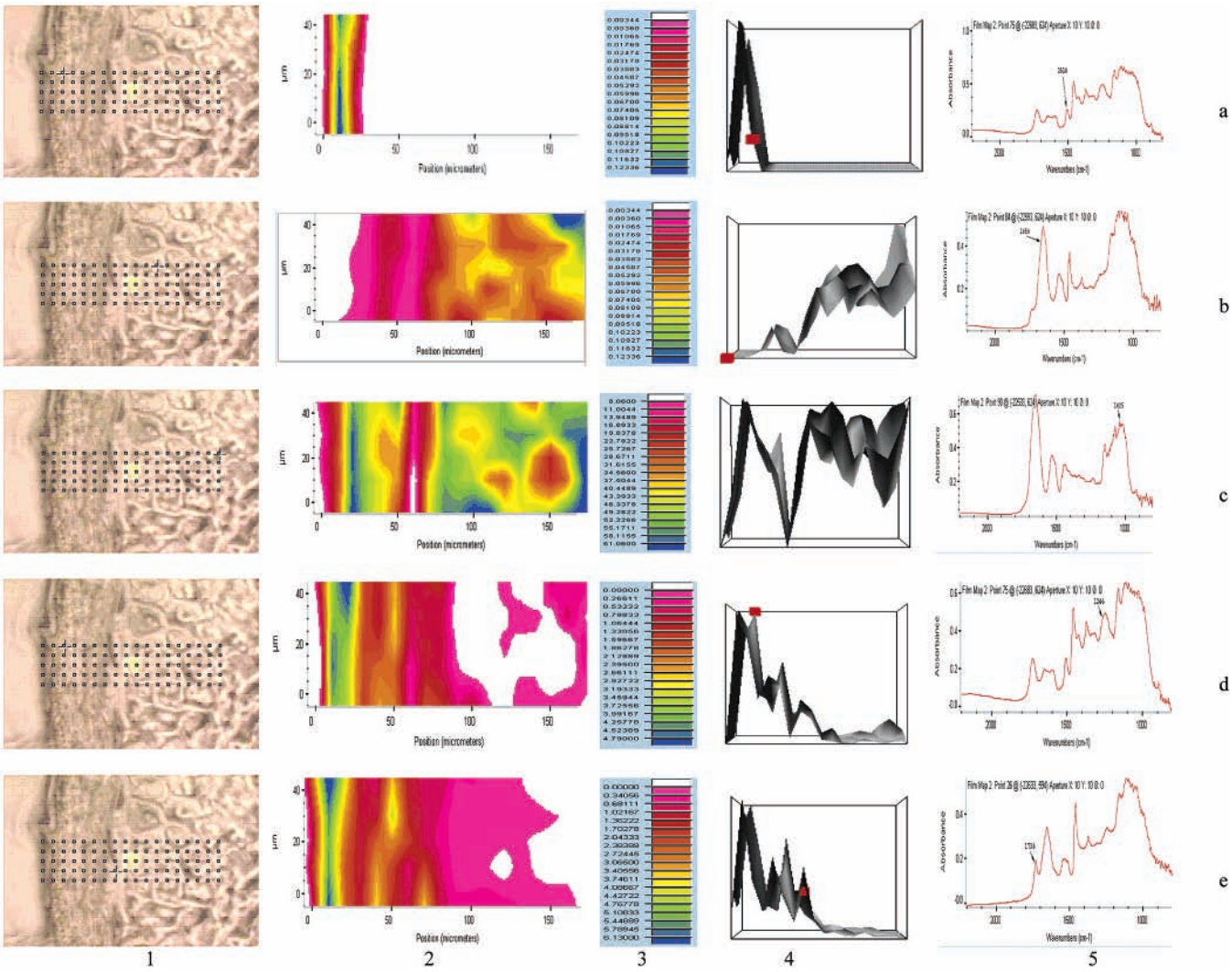

Figure 2. Functional group images of the barley tissue from the percarp, seed coat, aleurone, and endosperm (1, visible image; 2, chemical image; 3, chemical intensity; 4, 3D image; 5, spectra corresponding to the pixel at the cross-hair in the visible image). (**a**) Area under peaks centered at 1510 cm^{-1} showing lignin concentration and distribution. (**b**) Area under 1650 cm^{-1} peak (amide I) showing protein concentration and distribution. (**c**) Area under the peaks between 1180 and 1000 cm^{-1} (carbohydrates). (**d**) Area under peaks at 1246 cm^{-1} indicating cellulosic material concentration and distribution. (**e**) Area under peaks at 1738 cm^{-1} (C═O ester linkage) showing lipid concentration and distribution.

imaging or mapping without destruction of the intrinsic microstructures.

Microspectroscopic imaging by SR-FTIR can generate spatially localized chemical information without the need to homogenize the sample as done in traditional analytical chemistry. It combines chemical and spatial information. The chemical information (qualitative and quantitative analytical results) can be linked to structural information. The technique can be used to increase the fundamental understanding of plant structures at the cellular level and bring a new level of understanding of analytical information (*1*).

The objective of this study was to use this noninvasive bioanalytical technique, SR-FTIR microspectroscopy to chemically image the intrinsic structures of plant tissues at ultraspatial resolutions to reveal the plant feed structural chemistry information. The ultimate objective was to use this information to relate plant intrinsic microstructure to rumen biodegradation characteristics.

MATERIALS AND METHODS

Plant Tissue. Harrington barley (2000-BI-704) (a two row, broad, and diamond-shaped kernel barley bred for malting characteristics with an extremely rapid rate of fermentation) was grown in an university research plot near Saskatoon (Canada). The barley samples were supplied by B. Rossnagel, Crop Development Center (CDC), the University of Saskatchewan (Saskatoon, SK, Canada).

SR-FTIR Microspectroscopic Window Preparation. The plant samples were frozen at −20 °C on the objective disks in a microtome (Tissue Tech, NJ) and then cut into thin cross-sections (ca. 6 μm thickness) using a microtome at the Western College of Veterinary Medicine, University of Saskatchewan, Canada. The cross-sections of the plant tissues were rapidly transferred to BaF_2 windows (size, 13 mm × 1 mm disk; part number, 915-3015; Spectral Systems, NY) for transmission mode analysis in SR-FTIR microspectroscopic work. Several cross-sections were prepared within each BaF_2 window.

Photomicrograph of Cross-Sections of Plant Tissue. Photomicrographs of the cross-sections of the barley tissue (thickness, ca. 6−10 μm) were taken by a microscope with an attached digital camera from regular glass slides.

Synchrotron Light Source and SR-FTIR. This experiment was performed at the National Synchrotron Light Source in the Brookhaven National Laboratory (NSLS-BNL, NY) on beamline U10B. The spectroscopic images were recorded using a Nicolet Magna 860 FTIR (Thermo Nicolet, U.S.A.) equipped with a Continuum IR microscope (Spectra Tech, U.S.A.), mapping stage controller, 32× objective, and a mercury cadmium telluride (MCT-A) detector. The bench was

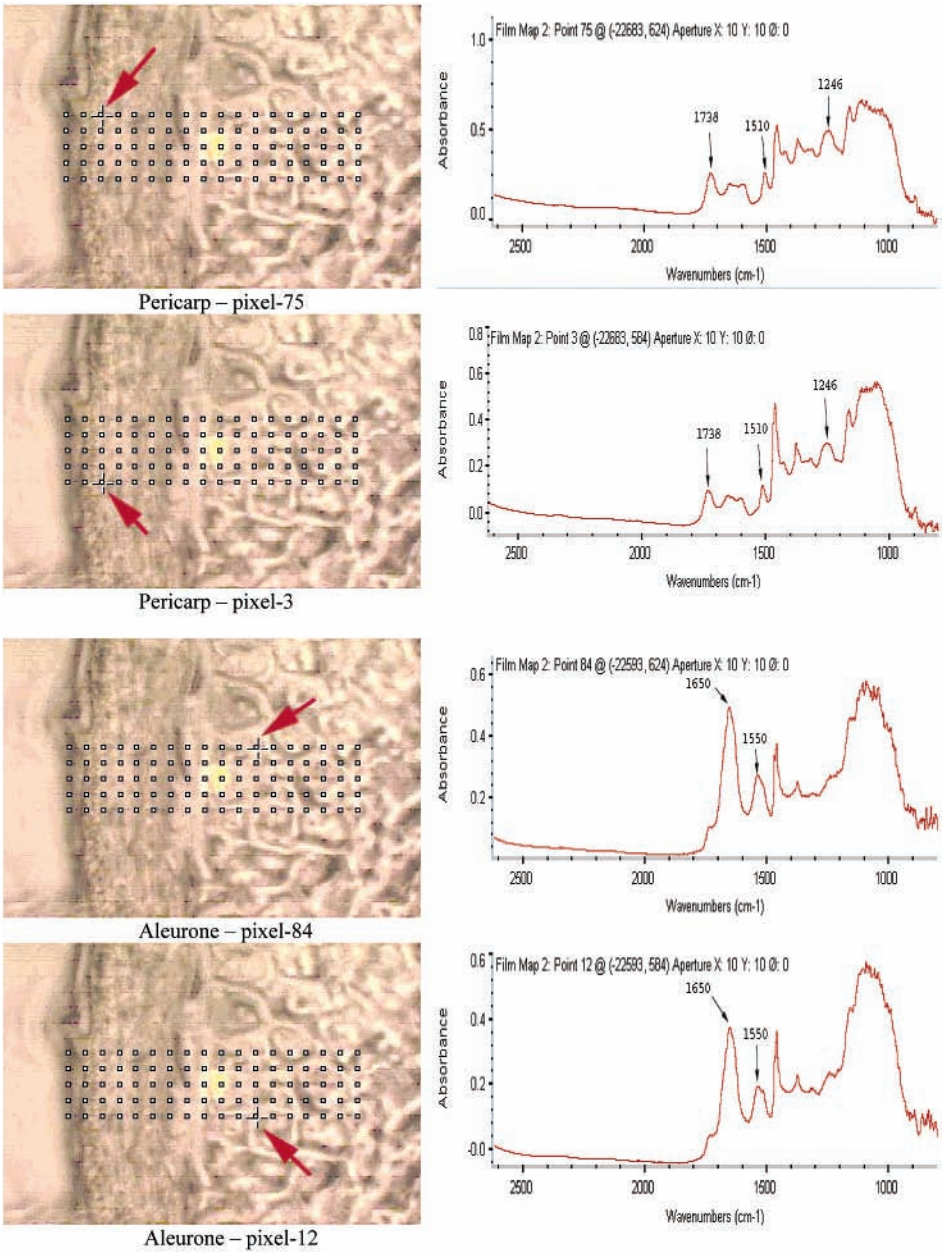

Figure 3. Spectra of pericarp and aleurone layer of barley seeds selected from the corresponding area from the visible images, showing that similar morphological parts exhibit similar spectral characteristics and chemical compositions.

configured with a synchrotron light beamline with an energy level of 800 MeV (U10B, NSLS-BNL). The spectra were collected in the mid-infrared range of 4000−800 cm^{-1} at a resolution of 4 cm^{-1} with 64 scans coadded and an aperture setting of ca. 10 μm × 10 μm. A background spectroscopic image file was collected from an area free of sample. The mapping steps were equal to the aperture size. Scanned visible images were obtained using a charge-coupled device camera linked to the infrared images.

Data Analysis and Chemical Imaging. The spectral data of the plant tissues were collected, corrected with the background spectrum, displayed in the absorbance mode, and analyzed using OMNIC software 6.0 (Spectra Tech). A baseline correction was applied to generate the final spectra. The SR-FTIR absorbance was expressed as Log (1/*R*). The data was displayed as either a series of spectroscopic images collected at individual wavelengths or a collection of infrared spectra obtained at each pixel position in the image.

Chemical imaging of functional groups - protein indicated by amide I (1650 cm^{-1}), lipid indicated by carbonyl C═O ester linkage band (1738 cm^{-1}), total carbohydrates (1180 to 1000 cm^{-1}), lignin (1510 cm^{-1}), cellulosic materials (1246 cm^{-1}) (*4*) as well as chemical component ratio (such as protein:total carbohydrate; cellulose:total carbohydrate)—in the intrinsic structures of the plant feeds were determined using the OMNIC software 6.0 (Spectra Tech) (*4*, *6*, *8*).

RESULTS AND DISCUSSION

Traditional Chemical Analysis vs Advanced Analytical Technique (SR-FTIR). To this point, there has been little research conducted with ultraspatially resolved chemical mapping or imaging of microstructures of plant tissues using SR-FTIR microspectroscopy. So far, only one paper from another research laboratory (*4*) has been found. Such information is important for a better understanding of plant tissue chemistry in relation to rumen biodegradation behaviors.

As mentioned previously, when using traditional "wet" chemical analysis, we are usually looking for a specific known component through homogenization of the plant tissue and separation of the components of interest from the complex matrix. Therefore, chemical structures and molecular characteristics of the intrinsic structures of the plant are destroyed during such processing, making it impossible to relate the

digestive function in animals to plant structures. For example, using wet chemical analysis, it was found that Harrington barley has a similar starch content as Valier barley; however, an in situ rumen study showed that Harrington barley has a different rumen degradation behavior than Valier barley (*9*). The predicted potential nutrient supply by the NRC-2001 and DVE/OEB models (*10*) also differs between the two types of barley (*9*). Why does traditional wet chemical analysis fail to detect such a biological difference? This is because the spatial origin and distribution of the starch in barley seeds is lost and destroyed during the sample processing for wet chemical analysis.

Ultraspatially Resolved Chemical Mapping of Plant Tissue. The chemical microstructure of barley seeds has been of interest in our laboratory (*11*, *12*) in regard to utilization for ruminants. Of particular concern have been its rapid degradation characteristics (*9*). **Figure 1** illustrates the intrinsic structure of barley tissue (cv. Harrington; 6 μm thickness cross-section) from the pericarp at the outside of the seed, to the seed coat, through to the aleurone layer and the endosperm. The pericarp forms the tough outer covering of the seed kernel and provides protection for the interior components. The seed coat is found between the pericarp and the aleurone layer. The aleurone cells play an important role during seedling development. The endosperm consists of cells filled mainly with starch granules.

Figure 2 represents color maps of functional groups of a cross-section of barley tissue through the pericarp, seed coat, aleurone, and endosperm area and single pixel spectra measuring an area as small as 10 μm $\times$ 10 μm of the sample. It shows visible and chemical images in false color representation of chemical component intensities, three-dimensional (3D) images, and spectra at various pixels. Using SR-FTIR microspectroscopy the distribution and relative concentration of the chemical components associated with the plant inherent structure were mapped.

Figure 2a shows the spatial lignin distribution and concentration of the area under peaks centered at 1510 cm^{-1}. This infrared image was taken from the region of the visible image outlined by the dotted area. The 1510 cm^{-1} band corresponds to the stretch associated with para-substituted benzene rings and can be associated with aromatic species present only in the pericarp of barley seeds.

Figure 2b shows the area under the 1650 cm^{-1} peak attributed to protein absorption (amide I). Amide I (1650 cm^{-1}) and amide II (1550 cm^{-1}) are characteristics of C═O and N−H bonds in the protein backbone and are indicators of the area of the sample where protein is present. **Figure 2b** shows that the pericarp region has no protein associated with it, and protein concentration is increased from the seed coat to the endosperm. The highest protein concentration is found in the subaleurone and endosperm layers. The area under the peaks between 1180 and 1000 cm^{-1} is plotted in **Figure 2c**. This area represents total carbohydrate absorption. This includes starch absorption in the endosperm and the structural carbohydrates (cellulose and hemicellulose) (1246 cm^{-1}) in the pericarp and the aleurone layers. The starch peak is centered at 1025 cm^{-1}. The 3D image in **Figure 2c** shows uneven distribution of total carbohydrate. Levels are high in the pericarp and aleurone and endosperm areas and very low in the seed coat. The area under the peaks centered at 1246 cm^{-1} indicates cellulose (*4*) (**Figure 2d**). The highest concentration is in the pericarp area, and a very low concentration is in the endosperm region (3D image). **Figure 2e** shows the lipid distribution at 1738 cm^{-1}. The band at 1738 cm^{-1} is due to the carbonyl group (C═O) stretching vibration in the ester linkage in the pericarp and aleurone layer. The

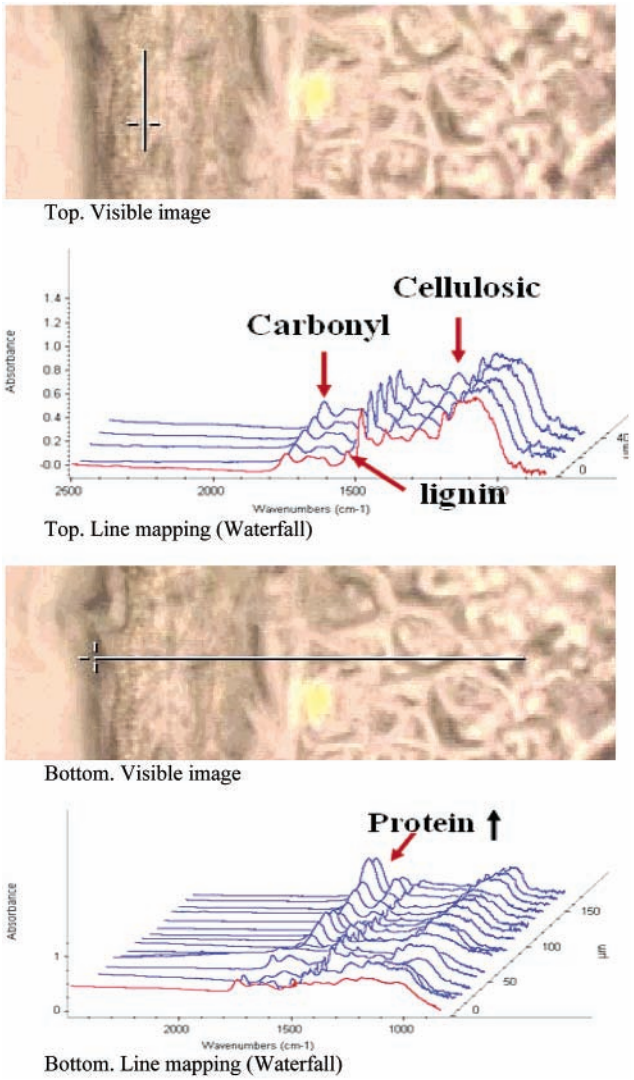

Figure 4. Line mapping shows that similar morphological parts have similar spectral characteristics indicating spatial chemical homogeneity (top), and different morphological parts have different spectral characteristics indicating spatial chemical heterogeneity of barley tissue (bottom).

aleurone and endosperm areas contain little lipid. The spectra on the right in each figure correspond to the pixel in the cross-hair and were selected to represent the value of the integrated peak. The represented spectra show a wide variety of spectral characteristics, which manifest the chemical composition in different morphological parts of the seed.

Figure 3 presents spectra of the pericarp and aleurone layers, showing that similar morphological parts exhibit similar spectral characteristics and chemical composition. The pericarp region contains a higher concentration of lignin (1510 cm^{-1}), cellulose (1246 cm^{-1}), and lipid (1738 cm^{-1}) materials and a low concentration of protein (1650 cm^{-1} for amide I band and 1550 cm^{-1} for amide II band). Contrary to that, the aleurone layer has practically no lignin and higher protein.

Figure 4 presents line mapping of the seed and again illustrates that similar morphological parts of the seed exhibit similar spectral characteristics. This indicates spatial chemical homogeneity in the seed and that different morphological parts exhibit different spectral characteristics, which indicates spatial chemical heterogeneity in the seed.

Figures 5 and **6** illustrate two peak area ratio images. **Figure 5** shows the peak area ratio of protein and carbohydrate and

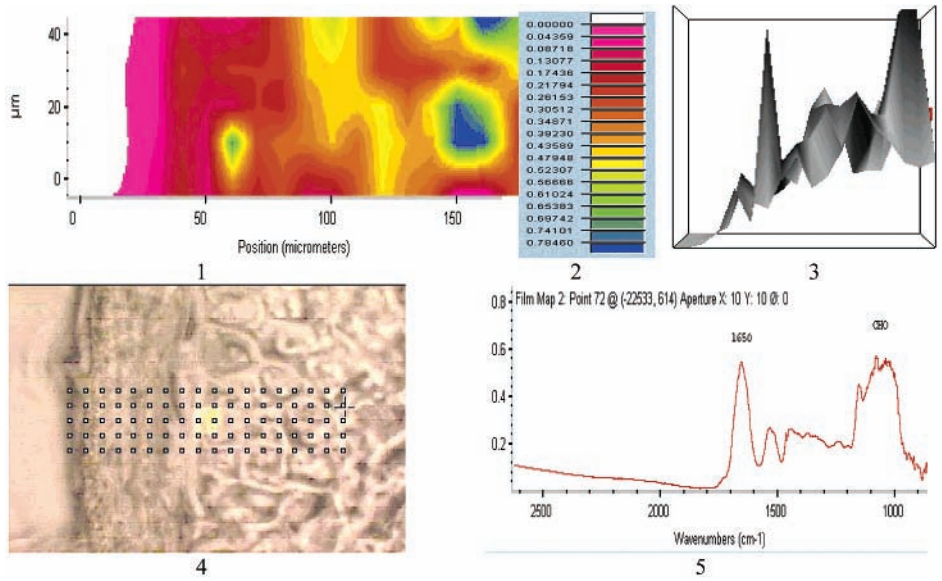

Figure 5. Peak area ratio—area under the 1650 cm^{-1} band divided by the area under the peaks between 1180 and 1000 cm^{-1} at each pixel—representing protein to total carbohydrate ratio in barley seed (1, chemical ratio image; 2, chemical intensity; 3, 3D image; 4, visible image; 5, spectra corresponding to the pixel at the cross-hair in the visible image).

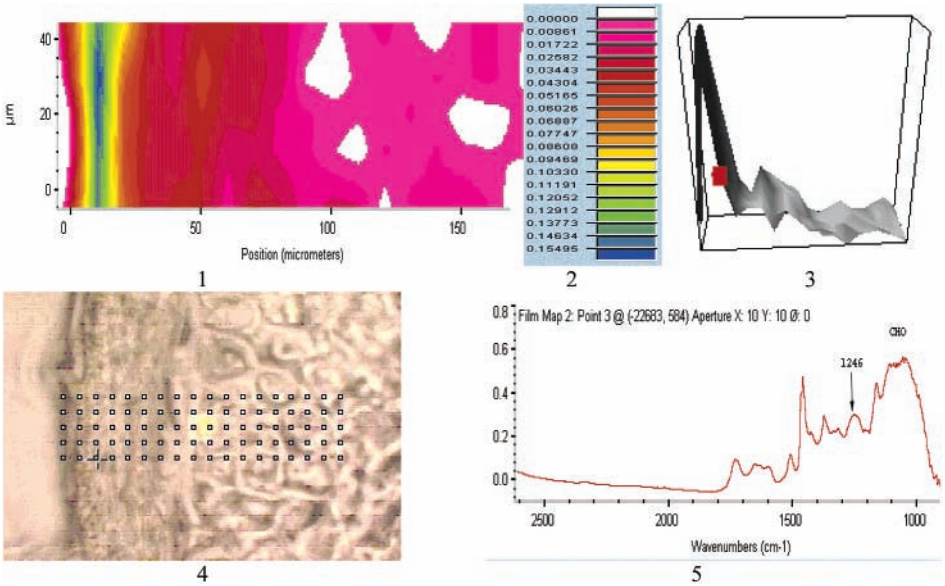

Figure 6. Peak area ratio—area under the 1246 cm^{-1} band divided by the area under the peaks between 1180 and 1000 cm^{-1} at each pixel—representing hemicellulose to total carbohydrate ratio in barley seed (1, chemical image; 2, chemical intensity; 3, 3D image; 4, visible image; 5, spectra corresponding to the pixel at the cross-hair in the visible image).

represents the distribution of the area under the 1650 cm^{-1} band divided by the area under the peaks between 1180 and 1000 cm^{-1} at each pixel. Using this ratio, any spectral intensity variation due to tissue thickness changes is eliminated. In this case, the image in **Figure 5** can be interpreted as the protein to total carbohydrate distribution. The spectra in the figure were chosen to represent this ratio. The results show that the highest ratio of protein to carbohydrate is in the aleurone and endosperm region. **Figure 6** shows the peak area ratio of cellulose (1246 cm^{-1}) to total carbohydrate (1180 to 1000 cm^{-1}). The results show that the highest ratio of cellulose to total carbohydrate is in the pericarp area.

The above work clearly shows that imaging chemical and functional group distribution across plant tissue at ultraspatial resolution at a cellular level can be accomplished using the FTIR microspectroscopy powered by synchrotron bright light. Such information could be analyzed for clues of the plant intrinsic structures in relation to biodegradation characteristics in animals. For example, the previous studies in our laboratory (*9*, *12*) showed that feed type barley (cv. Valier) and malting type barley (cv. Harrington) markedly differ in degradation behavior in ruminants. Harrington barley is higher in the rate and extent of rumen degradation than Valier barley. A high degradation of barley may result in digestive disorders in ruminants when feeding barley-based concentrate diets. Traditional wet chemical analysis methods cannot detect such biological differences. Using SR-FTIR microspectroscopy it has been found that the synchrotron infrared absorbance intensity of starch to protein ratio was different (4.12 vs 2.78 for Harrington and Valier barley, respectively) (unpublished data) indicating that the chemical matrix of microendosperm tissue is different. A lower starch to protein ratio in the microendosperm tissue of Valier barley implicates that starch granules in Valier barley have more proteins associated with. This may prevent Valier barley from

degrading fast and highly in the rumen. More research is needed on the chemical makeup of the intrinsic microstructure of plant tissues for a better understanding of their nutritive values for animals.

CONCLUSIONS

With SR-FTIR, the ultraspatial resolution was achievable, which allowed us to map individual parts of the plant structure in pixel-sized increments (10 μm) and allowed us to "see" plant tissue in a chemical sense on a cellular level. The results showed that with SR-FTIR, the chemical composition distribution of the plant tissues such as lignin, cellulose, protein, lipid, and total carbohydrate could be imaged. These images generated spatially localized chemical information and revealed chemical heterogeneity of the plant intrinsic structure. Such information can be analyzed for clues of the plant intrinsic structures in relation to biodegradation characteristics in animals.

ACKNOWLEDGMENT

We are grateful to Dr. Brian Rossnagel (The University of Saskatchewan) for supplying plant feed samples.

LITERATURE CITED

(1) Budevska, B. O. *Vib. Spectrosc.* **2002**, 3720−3732.
(2) Holman, H.-Y. N.; Bjornstad, K. A.; McNamara, M. P.; Martin, M. C.; McKinney, W. R.; Blakely, E. A. Synchrotron infrared spectromicroscopy as a novel bioanalytical microprobe for individual living cells: cytotoxicity considerations. *J. Biomed. Opt*. **2002**, *7*, 1−10.
(3) Miller, L. M.; Carlson, C. S.; Carr, G. L.; Chance, M. R. A Method for Examining the Chemical Basis for Bone Disease: Synchrotron Infrared Microspectroscopy. *Cell. Mol. Biol.* **1998**, *44*, 117−127.
(4) Wetzel, D. L.; Eilert, A. J.; Pietrzak, L. N.; Miller, S. S.; Sweat, J. A. Ultraspatially resolved synchrotron infrared microspectroscopy of plant tissue in situ. *Cell. Mol. Biol*. **1998**, *44*, 145−167.
(5) Miller, L. M. The impact of infrared synchrotron radiation on biology: past, present, and future. *Synchrotron Radiat. News* **2000**, *13*, 31−37.
(6) Miller, L. M. Infrared Microsperctroscopy and Imaging. http://nslsweb.nsls.bnl.gov/nsls/pubs/nslspubs/imaging0502/irxrayworkshopintroduction.ht, October 2002.
(7) Marinkovic, N. S.; Huang, R.; Bromberg, P.; Sullivan, M.; Toomey, J.; Miller, L. M.; Sperber, E.; Moshe, S.; Jones, K. W.; Chouparova, E.; Lappi, S.; Franzen, S.; Chance, M. R. Center for Synchrotron Biosciences' U2B beamline: an international resource for biological infrared spectroscopy. *J. Synchrotron Radiat*. **2002**, *9*, 189−197.
(8) Himmelsbach, D. S.; Khalili, S.; Akin, D. E. FT-IR microspectroscopic imaging of flax (linum usitatissimum L.) stems. *Cell. Mol. Biol.* **1998**, *44*, 99−108.
(9) Yu, P.; Meier, J.; Christensen, D. A.; Rossnagel, B.; McKinnon, J. J. Using the NRC model and the DVE/OEB system to evaluate nutritive values of Harrington and Valier barley for ruminants. *Anim. Feed Sci. Technol*. **2003a**, *106*, 45−60.
(10) Yu, P.; Christensen, D. A.; McKinnon, J. J. Comparison of the National Research Council-2001 Model with the Dutch System (DVE/OEB) in the Prediction of Nutrient Supply to Dairy Cows from Forages. *J. Dairy Sci.* **2003b**, *86*, 2178−2192.
(11) Yu, P.; McKinnon, J. J.; Christensen, C. R.; Drew, M.; Christensen, D. A. Synchrotron Fourier Transform Infrared Microspectroscopy (S-FTIR) as a Novel Bioanalytical Microprobe for Ultrastructural Matrix of Barley Endosperm Tissue. *Proceedings of the 5th CLS Users Meeting and Synchrotron Workshop−Applications of Synchrotron Radiation in the Biological/Life Sciences. Canadian Light Sources*; University of Saskatchewan: Saskatoon, Canada, 2002; p 39.
(12) Yu, P.; McKinnon, J. J.; Christensen, C. R.; Drew, M.; Christensen, D. A. Exploring ultrastructural matrix of barley endosperm tissue between malting-type and feed-type barley using synchrotron Fourier transform infrared microspectroscopy. *Cell. Mol. Biol.* **2003c**, in review.

Received for review June 19, 2003. Revised manuscript received July 25, 2003. Accepted July 30, 2003. This research has been supported by grants from the Saskatchewan Agricultural Development Fund (ADF) and the Natural Sciences and Engineering Research Council of Canada (NSERC). The National Synchrotron Light Source in Brookhaven National Laboratory (NSLS-BNL, New York) is supported by the U.S. Department of Energy contract DE-AC02-98CH10886.

JF034654D